

Electronic Supplementary Information

**CO₂-philic ferrocene-based porous organic polymer for solar-driven
CO₂ conversion from flue gas**

Zhou Fang,^{a,b} Yuqi Wang,^{a,b} Yue Hu,^{a,b} Bing Yao,^{a,b} Zhizhen Ye,^{a,b} Xinsheng Peng^{a,b,}*

^aState Key Laboratory of Silicon Materials and Advanced Semiconductor Materials,
School of Materials Science and Engineering, Zhejiang University, Hangzhou 310027,
P. R. China.

^bWenzhou Key Laboratory of Novel Optoelectronic and Nanomaterials, Institute of
Wenzhou, Zhejiang University, Wenzhou 325006, Zhejiang, P. R. China.

^{a,b,*} Email: pengxinsheng@zju.edu.cn

Experimental section

Materials

All chemicals were purchased from commercial sources and used without further treatment: 1,1'-ferrocenedicarboxaldehyde (Fc, C₁₂H₁₀FeO₂, Shanghai Aladdin Biochemical Technology Co., Ltd., 98%), 2-(4-aminophenyl)-1H-benzimidazol-5-amine (BIA, C₁₃H₁₂N₄, Shanghai Aladdin Biochemical Technology Co., Ltd., 98%), dimethyl sulfoxide (DMSO, C₂H₆OS, Chengdu Kelong Chemical Reagent Co., Ltd., AR), tetrahydrofuran (THF, C₄H₈O, Chengdu Kelong Chemical Reagent Co., Ltd., AR), acetone (CH₃COCH₃, Chengdu Kelong Chemical Reagent Co., Ltd., AR), methanol (CH₃OH, Chengdu Kelong Chemical Reagent Co., Ltd., AR), ethanol (C₂H₅OH, Chengdu Kelong Chemical Reagent Co., Ltd., AR), tetrabutylammonium bromide (TBAB, C₁₆H₃₆BrN, Shanghai Aladdin Biochemical Technology Co., Ltd., 99%, AR), Styrene oxide (SO, C₈H₈O, Shanghai Aladdin Biochemical Technology Co., Ltd., 98%), Epichlorohydrin (ECH, C₃H₅ClO, Shanghai Macklin Biochemical Technology Co., Ltd., AR), Epibromohydrin (EBH, C₃H₅BrO, Shanghai Macklin Biochemical Technology Co., Ltd., AR), 1,2-epoxyhexane (C₆H₁₂O, Shanghai Aladdin Biochemical Technology Co., Ltd., >96%), cyclohexene oxide (C₆H₁₀O, Shanghai Aladdin Biochemical Technology Co., Ltd., 98%), 2,3-epoxy-1-phenylpropane (C₉H₁₀O, Shanghai Haohong Biochemical Technology Co., Ltd., 98%), (S)-((benzyloxy)-methyl)oxirane (C₁₀H₁₂O₂, Shanghai Haohong Biochemical Technology Co., Ltd., 99%), terephthalaldehyde (TPA, C₈H₆O₂, Shanghai Macklin Biochemical Technology Co., Ltd., 98%), toluene (C₇H₈, Chengdu Kelong Chemical Reagent Co., Ltd., AR), sodium sulfate (Na₂SO₄, Shanghai Macklin Biochemical Technology Co., Ltd., AR), Nafion 117 solution (5 wt%, Shanghai Aladdin Biochemical Technology Co., Ltd.), iso-propanol (Shanghai Macklin Biochemical Technology Co., Ltd., AR). The ultrapure water of 18.2 MΩ used throughout the experiments was produced by a Millipore direct-Q system (Millipore).

Preparation of Fc-POPs

Firstly, BIA (0.41 mmol) and Fc (0.41 mmol) were suspended in anhydrous DMSO (40 mL). Then the solution was then encapsulated in ampoule bottle and degassed by freeze-pump-thaw technique for three times in the liquid nitrogen bath. Finally, the bottle was evacuated to an internal pressure of 150 mtorr. The reaction was heated to 150 °C for 72 h to obtain a black solid, which was filtered and washed with THF, acetone and methanol for three times. Further purification of the crude product was conducted by exhaustive Soxhlet extraction with THF for 24 h and methanol for 24 h. The final product was dried in a vacuum oven for 12 h at 80 °C to afford black powder. The Fc-POPs productivity is over 90%.

Preparation of TPA-POPs

BIA (0.41 mmol) and TPA (0.41 mmol) were suspended in anhydrous DMSO (40 mL). The solution was then encapsulated in ampoule bottle and degassed by freeze-pump-thaw technique for

three times in the liquid nitrogen bath. Finally, the bottle was evacuated to an internal pressure of 150 mtorr. The reaction was heated to 150 °C for 72 h to obtain a light orange solid, which was filtered and washed with THF, acetone and methanol for three times. Further purification of the crude product was conducted by exhaustive Soxhlet extraction with THF for 24 h and methanol for 24 h. The final product was dried in a vacuum oven for 12 h at 80 °C to afford light orange powder.

Characterization

Powder X-ray diffraction patterns (PXRD) were collected on X-pert Powder diffractometers (PANalytical instrument) using Cu K α ($\lambda=1.5406$ Å) radiation at 0.02 degree step. Scanning electron microscopy (SEM) images were collected using a SU-4800 (Hitachi, Japan), assisted with accessories of X-ray energy dispersive spectrometer (EDS) analysis. Transmission electron microscopy (TEM) images assisted with EDS analysis were taken on HT-7700 TEM (Hitachi, Japan). The cross polarization magic angle spinning carbon-13 nuclear magnetic resonance (CPMAS ^{13}C NMR) measurements were carried out with a Avance III HD (Bruker) spectrometer operating at 400 MHz. The Fourier-transform infrared spectroscopy (FTIR) spectra were recorded using a KBr pellets as background in the range of 4000-400 cm^{-1} on TENSOR 27 spectrometer (Bruker). X-ray photoelectron spectroscopy (XPS) spectra were performed on AXIS SUPRA (Krato) with Al K α irradiation at $\theta=90^\circ$ for X-ray sources. The binding energies were calibrated using the C 1s peak at 284.8 eV. Thermogravimetric analysis was carried out on TA-Q500 thermogravimetric analyzer under N $_2$ atmosphere. Nitrogen adsorption measurements were collected at 77 K on AUTOSORB-1-C (QUANTACHROME). Carbon dioxide sorption isotherms were measured by using the automatic volumetric adsorption equipment at 298 K on ASAP 2020 (Micromeritics). UV/vis/NIR spectrometer analyses were recorded on Agilent Cary 5000 (Agilent). NH $_3$ temperature programmed desorption (NH $_3$ -TPD) and CO $_2$ temperature programmed desorption (CO $_2$ -TPD) was carried out on a TP-5080 analyzer (Xianquan) to detect the Lewis acid sites and Lewis base sites, respectively. The signals were recorded by monitoring the desorbed gas with a TCD detector. To determine the content of Fe atoms in Fc-POPs, inductively coupled plasma optical emission spectrometer (ICP-OES) was conducted on 730-ES (Varian). On account of high chemical and heating stability of Fc-POPs structure in acid solution, the samples were first through a pyrolysis process (873 K, 6 h), and then, the obtained powders were dissolved in aqua regia and diluted them to the suitable concentration for ICP detection. The content of N was determined by elemental analyzer EA3000 (Euro Vector). PL emission spectra of Fc-POPs powders were conducted on fluorescence spectrophotometer (OmniFluo990). Photoelectric properties of Fc-POPs catalyst were investigated using electrochemical method with a CHI 760E electrochemical workstation in three-electrode configuration. It was achieved in a Na $_2$ SO $_4$ (0.5 M) electrolyte solution in a quartz cell, where the Fc-POPs served as the working electrode, Pt electrode as the counter electrode, and Ag/AgCl electrode as the reference electrode. The working electrode of Fc-POPs catalyst ink was prepared by dispersing 5 mg of catalyst material in a mixture of 50 μl Nafion 117 solution and 950 μl iso-propanol with the assistance of sonication for 30 min. Then, the working electrodes were

prepared by drop-drying 100 μl of catalyst ink onto ITO glass to cover an area of 1 cm^2 (loading: 0.5 $\text{mg}\cdot\text{cm}^{-2}$).

Photothermal Characterization: The temperature of solid-state catalysts and CO_2 cycloaddition reaction systems dependence on light irradiation intensity and time were recorded via a FLIR-E5-xt camera (FLIRSystems, Inc.). Simulated sunlight was mimicked by a CELPE300-3A Xenon lamp (PerkinElmer, 300W) with a standard AM 1.5G optical filter, and the optical intensity was confirmed with an optical power meter CEL-NP2000-2 (CEAUlight). During the temperature measurements, photos of catalysts or reaction reactors' temperature were recorded in a certain interval, and the average temperature was determined from infrared images disposed by FLIR Tool.

Catalytic performance measurement

Photo-driven catalytic cycloaddition with epoxide in pure CO_2 : Reaction of cycloaddition with CO_2 and styrene oxide was chosen as probe reaction. In general, 10 mg catalysts, 0.25 mmol co catalyst (TBAB) and 12.5 mmol SO was added in a 20 mL sealed Schleck tube. The reactor was purged with pure CO_2 and vacuumed for several times to allow pure CO_2 atmosphere for the reaction. Then the catalytic cycloaddition reaction was carried out at designed light irradiation (from 0 W/cm^2 to 0.4 W/cm^2) with a Xe lamp. The reaction system sufficient contacted with gas via continuously stirring (400 rpm). The CO_2 pressure was kept under 1 bar with steady gas flow during the whole reaction. Typically, the catalytic reactions were last for 8 h. After CO_2 cycloaddition reaction, the mixture solution after catalysis needed centrifugation (10000 rpm, 10 min) to separate the catalyst from solution. Supernates were diluted in toluene and extracted by deionized water for several times in order to remove the residual TBAB. Subsequently, the solutions were required to add anhydrous Na_2SO_4 to eliminate remnant water in tested samples. After that, the solutions were filtrated and added dodecane as internal standard before investigated by Gas Chromatography (GC) analyses, which were performed on an equipment Agilent GC 6891 instrument with FID detector with HP-5 capillary column. The substances were verified by gas chromatograph-mass spectrometer (GC/MS, Agilent 7890B-5977A). In addition, the Fc-POPs catalysts after catalysis were demanded to be washed by ethanol for several times, collected and dried in vacuum oven overnight for recyclability test. However, when measure kinetic curves about CO_2 cycloaddition catalytic activity, reaction solution was taken out in certain time intervals, purified with filtration and then measured by GC.

Photo-driven catalytic cycloaddition with epoxide in dilute CO_2 : A series of 1 bar diluted CO_2 (15 vol%, 33 vol%, 50 vol%, 75 vol%), which were balanced with N_2 in volume, were used for CO_2 cycloaddition reaction, and other catalytic conditions were the same.

Conventional heating catalytic cycloaddition with epoxide in pure CO_2 : The tests were conducted with similar procedure compared to photo-driven catalytic cycloaddition reaction. The temperatures were identical to the corresponding light intensity via setting the temperature.

Recyclability investigation: After the reaction of CO_2 cycloaddition, the catalyst was separated by centrifugation and washed with ethanol for several times and dried overnight in vacuum oven. The

reused catalysts were recycled for the next cyclic reaction. The same procedure was repeated ten times and six times to test the recyclability and stability of Fc-POPs in pure and diluted CO₂ atmosphere while other conditions are identical. The yield of SC was determined by GC. After circulations, the catalysts were collected and dried for XRD, SEM and TEM examination to further confirm the stability of catalysts.

Turnover frequency: TOF value is determined by Equation S1-2, which is the essential parameter to evaluate the performance of Fc-POPs catalysts.

Equation S1: $TOF = TON \text{ value} / \text{reaction time (h)}$

Equation S2: $TON = \text{product (mmol)} / \text{active sites (mmol)}$

where the number of active sites were confirmed by ICP results in Table S1.

Catalytic activity: The activity of catalyst is determined by Equation S3. The value demonstrates the catalytic efficiency for the whole catalyst.

Equation S3: $\text{Value of catalytic activity} = \text{output of product (mmol)} / \text{weight of catalyst (g)}$.

Additional Figures and Tables



Fig S1. Image of the synthesized Fc-POPs (black powders).

Table S1. ICP results and elemental analysis of Fc-POPs catalysts.

Content of Fe (mmol/15mg) ^a	The content of N (mmol/15mg) ^b	Ratio of mol (Fc) and mol (BIA)
0.032067	0.130531	0.9827 \approx 1

^a The content of Fe was determined by ICP test.

^b The content of N was determined by elemental analyzer.

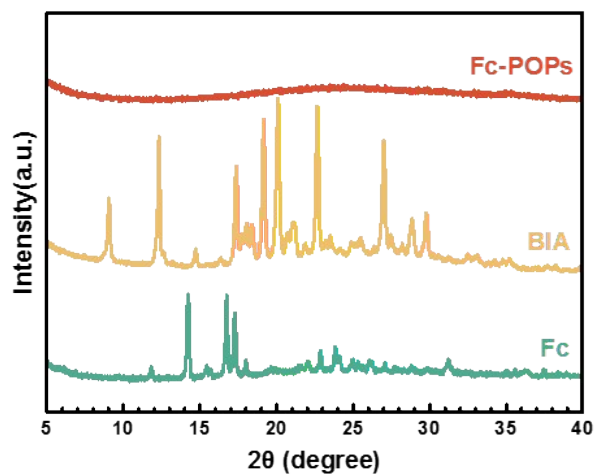


Fig S2. XRD patterns of Fc, BIA and Fc-POPs.

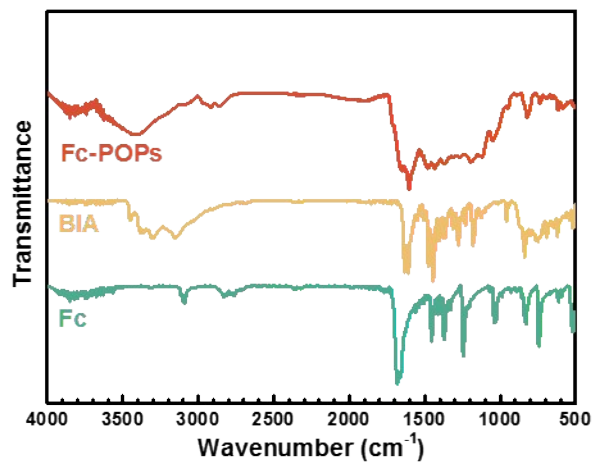


Fig S3. FTIR spectra of Fc, BIA, Fc-POPs.

Table S2. The CO₂ uptake for the cycloaddition reaction with epoxides catalyzed by various POP-based catalytic systems.

entry	catalyst	CO ₂ uptake (mg/g) ^a	reference
1	ImIP@TT-COF	22.88	[1]
2	COP-222	29.44	[2]
3	Bp-Zn@MA	37.4	[3]
4	IT-POP-1	42	[4]
5	PDVB-[AlTMG]Br-0.2	42.24	[5]
6	HPILs-Cl-2	44	[6]
7	1-Mn	45.91	[7]
8	POP-PBH	48.29	[8]
9	Co-HIP	51.04	[9]
10	IPOP1-XL	52	[10]
11	[HCP-CH ₂ -Im][Cl]	53.24	[11]
12	Zn-Por-PiP	53.24	[12]
13	ZnTPP/QA-azo-PiP ₁	56.32	[13]
14	Fe ₃ O ₄ @QP-CTP	57	[14]
15	Py@MA	58.52	[15]
16	Co/POP-TPP	58.67	[16]
17	DB-Tp	61.6	[17]
18	P-POF-Zn	67.3	[18]
19	PRP-1	71	[19]
20	Cr-CMP	71.7	[20]
21	HMP-TAPA	77	[21]
22	Co-CMP	79.3	[22]
23	ZPOF-500-30	81.4	[23]
24	TBB-BPY-Co	83.31	[24]
25	HIP-Br-2	83.6	[25]
26	HIP-Cl(3)-OH	88.88	[26]
27	Co-Por-POP-2	90.16	[27]
28	Co-Phen-POP	93.21	[28]
29	Al-Por-POP-2	94.5	[29]
30	CPP-IL0.05	97.8	[30]
31	HIP-Cl-1	101.2	[25]
32	Co@PAN-TDP	105	[31]
33	Al-Por-POP-1	109.2	[29]
34	HCP-TPP-Co-HZ	111	[32]
35	Fc-POP	111.6	This work

^a Volumetric CO₂ adsorption at 298 K, p/p₀=1.

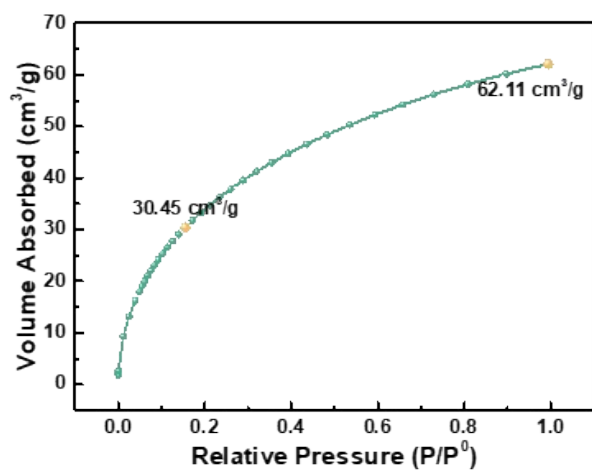


Fig S4. CO₂ adsorption isotherm of Fc-POPs at 298 K.

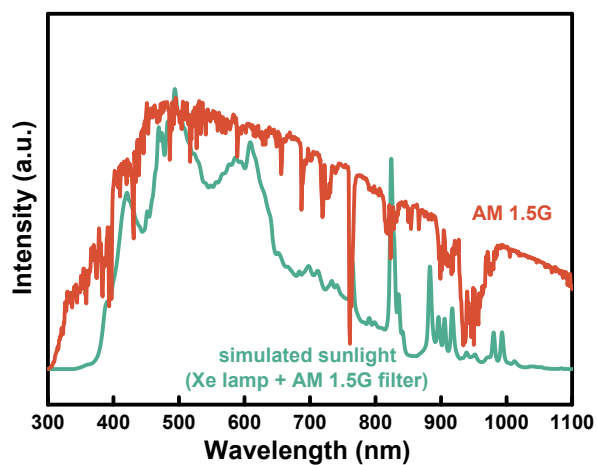


Fig S5. Optical spectra of referenced solar irradiation (red line) and simulated sunlight (green line).

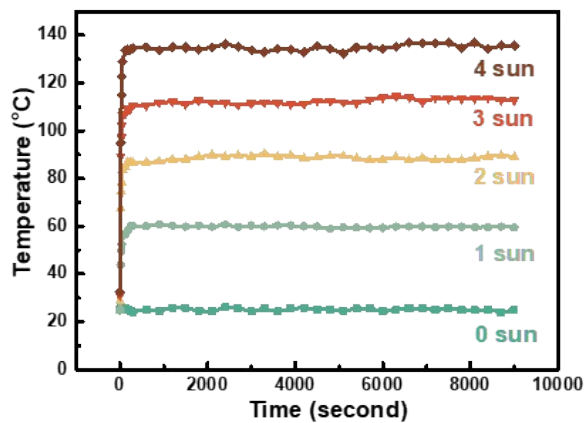


Fig S6. The temperature of solid-state powder (5 mg Fc-POPs) depend on time with diverse light

irradiation (0-0.4 W/cm²).

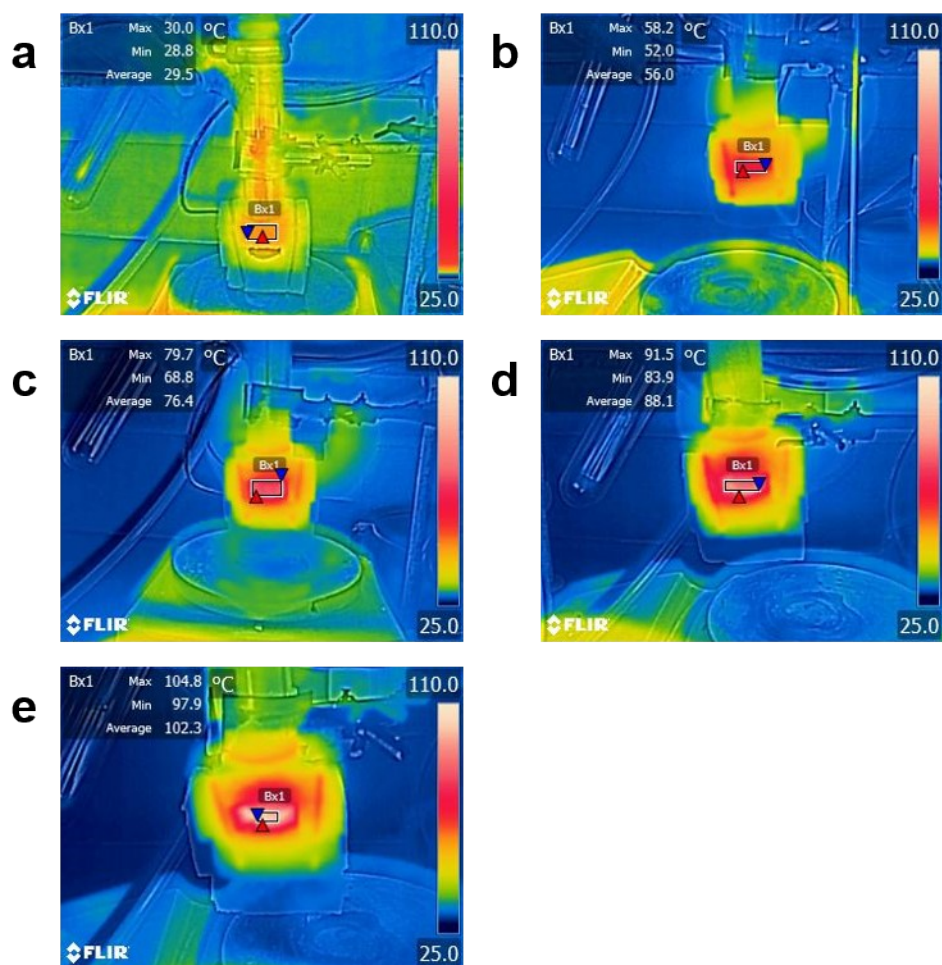


Fig S7. The FLIR photos of reaction systems under various simulated sunlight intensities. a) dark environment; b) 0.1 W/cm²; c) 0.2 W/cm²; d) 0.3 W/cm²; e) 0.4 W/cm². Reaction conditions: 10 mg Fc-POPs, 12.5 mmol SO, 0.25 mmol TBAB, 1 bar CO₂.

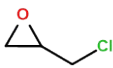
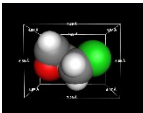
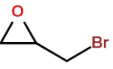
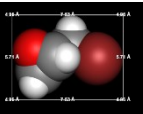
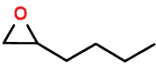
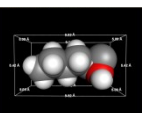


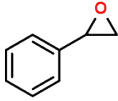
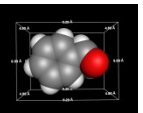
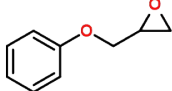
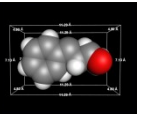
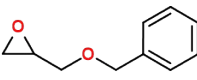
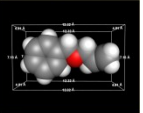
Table S3. Cycloaddition reaction of CO₂ with styrene oxide catalyzed by different catalysts ^a.

entry	catalyst	Yield (%) ^b
1	Fc	28.64
2	BIA	19.07
3	Fc+BIA	47.1
4	TBAB	14.29
5	Fc-POPs	94.7
6	TPA	27.45
7	TPA-POPs	33

^a Reaction conditions: 12.5 mmol SO, 10 mg catalyst, 0.25 mmol TBAB, CO₂ 1 atm, 8 h, 0.3 W/cm².

^b Catalytic reaction product was analyzed and identified by gas chromatography (GC).

Table S4. Catalytic cycloaddition reaction of CO₂ and epoxides with diverse substrates over Fe-POPs ^a.

entry	substrate	3D dimension ^b	molecular size ^c	Yield (%) ^d
1			7.29×5.58×4.97Å ³	> 99
2			7.53×5.71×4.96Å ³	> 99
3			9.92×5.42×5.10Å ³	33.35
4			6.72×6.95×5.10Å ³	48.5
5			9.20×6.99×4.80Å ³	94.7
6			11.29×7.13×4.80Å ³	trace
7			12.32×7.16×4.81Å ³	trace

^a Reaction conditions: 12.5 mmol SO, 10 mg catalyst, 0.25 mmol TBAB, CO₂ 1 atm, 8 h, 0.3 W/cm².

^b 3D dimension structures were determined by Chem Draw.

^c molecular sizes of substrates were calculated on the theoretical basis of Hu[33].

^d Catalytic reaction product was analyzed and identified by gas chromatography.

Table S5. A list of catalytic performance of reported POP-based catalysts for the cycloaddition with styrene oxide and co-catalyst in pure CO₂ atmosphere.

catalyst	Co-catalyst	Reaction time (h)	Temperature (°C)	Pressure (bar)	Yield (%)	TOF (h ⁻¹)	Ref.
Co/POP-TPP	TBAB	48	50	1	74.2	7.13	[16]
Zn@SBMMP	TBAB	4	90	20	97	51	[34]
1-Mn	TBAB	4	80	20	44	88	[7]
Al-Por-POP-2	TBAB	48	25	1	72.8	49.96	[29]
HMP-TAPA	TBAB	6	80	6	81	64.33	[21]
Co-Phen-POP	TBAB	48	25	10	64.8	248.81	[28]
Py-Zn@MA	ZnBr ₂	12	130	20	97	42	[15]
Co-Por-POP-2	TBAB	48	25	1	51.8	14.84	[27]
DB-Tp	TBAB	72	50	1	96	1.11	[17]
PRP-1	TBAB	72	60	1	66	/	[19]
1-Cr	TBAB	6	100	20	82	49.83	[35]
IPOP1-XL	TBAB	36	35	1	99	28.64	[10]
HPILs-Cl-2	TBAB	9	70	1	88	/	[6]
Cu/POP-Bpy	TBAB	48	80	1	86.2	3.59	[36]
TBB-BPY-Co	TBAB	48	25	10	66.7	240.85	[24]
DTBBQ-CMP	TBAB	48	60	1	99	35.71	[37]
Cr-CMP	TBAB	48	25	1	51.6	2.4	[20]
COF-salen-Co	TBAB	8	100	20	78	246	[38]
HCP-TPP-Co-HZ	TBAB	48	25	1	71	54.48	[32]
Zn@MA-POP	TBAB	8	250 W Xe lamp	1	91	/	[39]
Co-BD-COF	TBAB	24	40	1	11	0.23	[40]
Fc-POPs	TBAB	8	3 sun (~88.7°C)	1	94.7	71.63	This work

Table. S6 A list of catalytic performance of reported catalysts for the cycloaddition with styrene oxide in diluted CO₂.

entry	Catalyst/weight	CO ₂ (volume%/pressure)	Reaction time (h)	Temperature (°C)	Yield (%)	Ref.
1	Py-Zn@MA/20mg	20%/30 bar	12	130	90	[15]
2	Bp-Zn@MA/20 mg	20%/20 bar	6	100	89	[3]
3	ImIP@TT-COF/30 mg	15%/1 bar	48	120	66	[1]
4	HIP-Br-2/133mg	15%/1 bar	120	55	89	[25]
5	HIP-Br-2/33mg	15%/1 bar	48	120	40	[25]
6	HIP-Cl-2/30mg	15%/1 bar	48	120	34	[25]
7	PDVB-[AITMG]Br- 0.2/50 mg	15%/1 bar	48	100	99	[5]
8	Fc-POPs/15 mg	15%/1 bar	24	3 sun (T~88.7°C)	69	This work
9	Fc-POPs/15 mg	15%/1 bar	24	4 sun (T~102°C)	93	This work

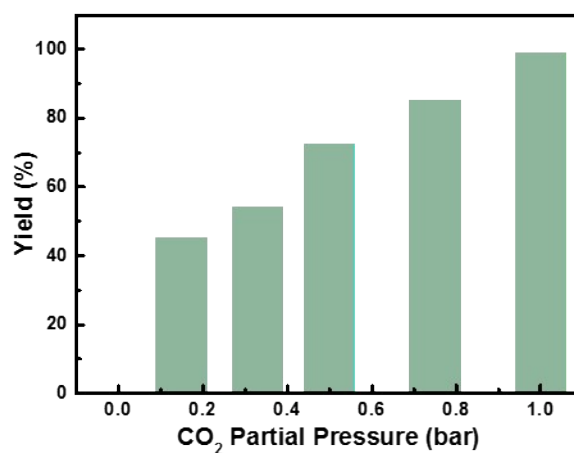


Fig S8. The yield of SC depends on the diverse CO₂ partial pressure under 0.3 W/cm² light irradiation for 12 h.

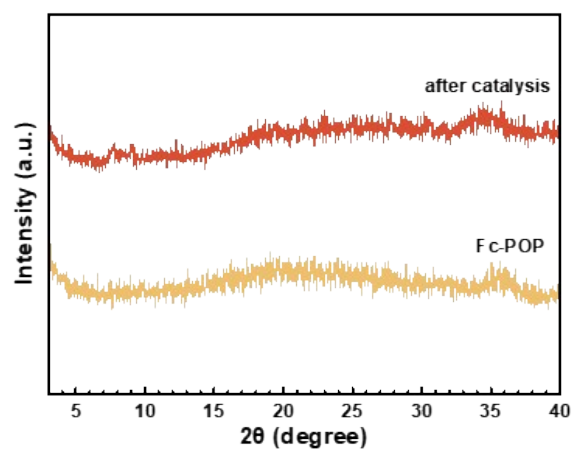


Fig S9. XRD patterns of Fc-POPs before and after catalysis.

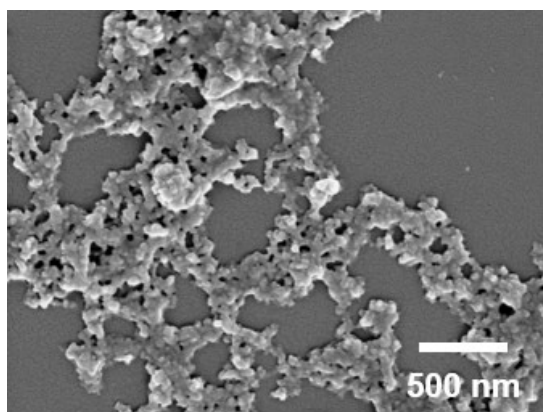


Fig S10. SEM images of Fc-POPs after recyclability test.

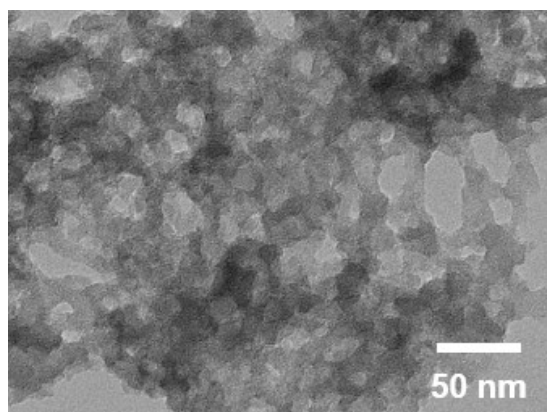


Fig S11. TEM images of Fc-POPs after recyclability test.



Fig S12. Images of optical intensities (a) in the darkness and (b) under ambient light through optical power meter.

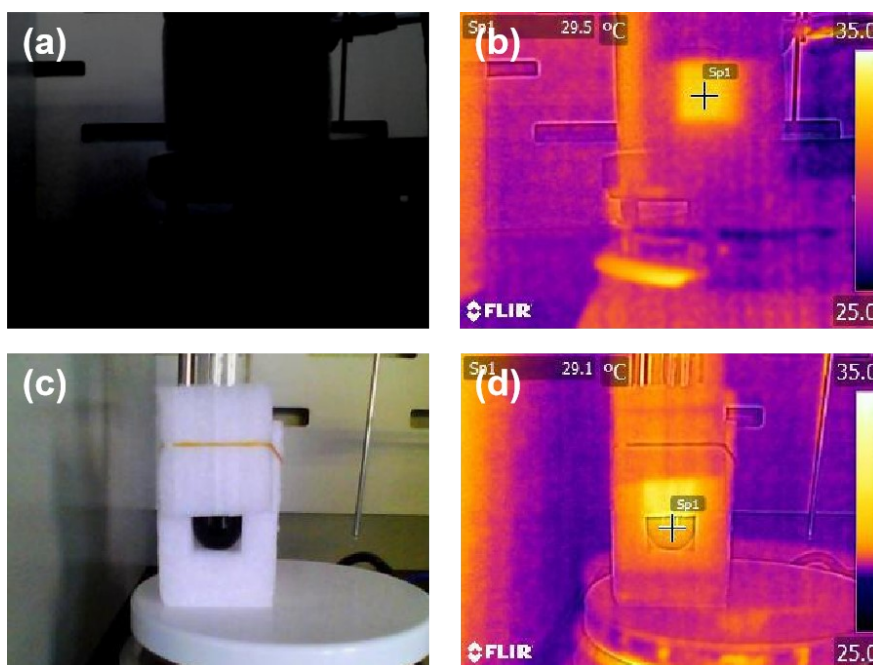


Fig S13. The images (a) and FLIR photos (b) of reaction systems in the darkness; the images (c) and FLIR photos (d) of reaction systems under ambient light.

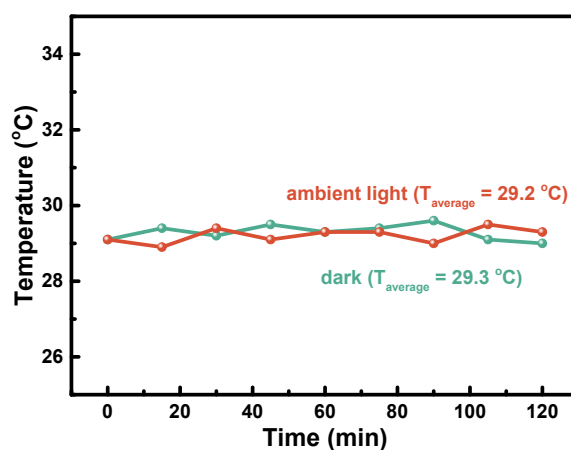


Fig S14. Temperatures of reaction system under ambient light and in the darkness, lasting for 120 min.

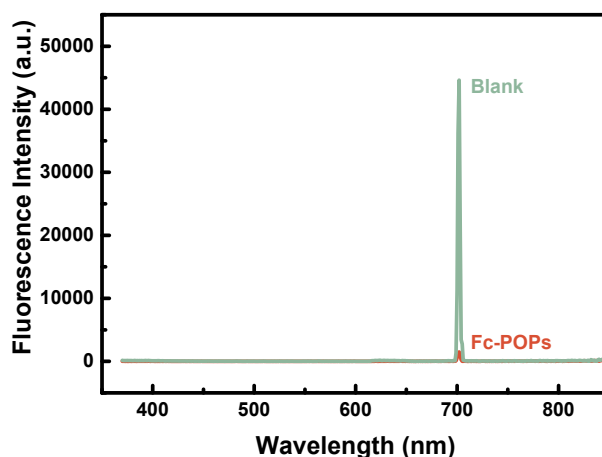


Fig S15. Fluorescence spectra of Fc-POPs powders with λ_{exc} at 350 nm.

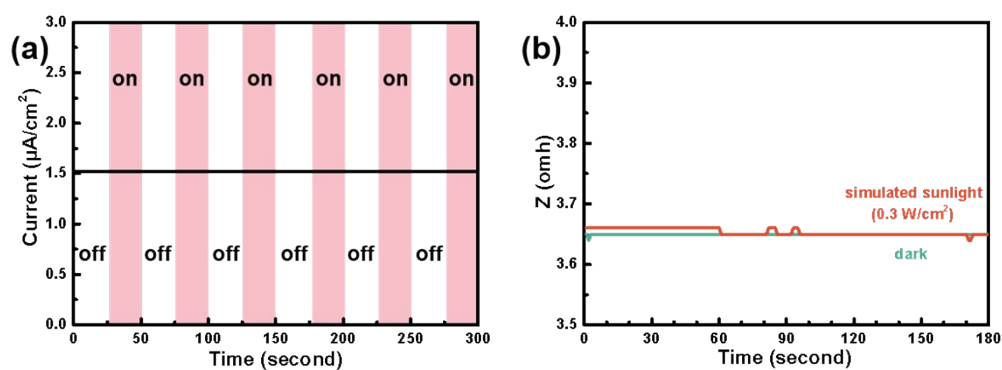


Fig S16. (a) Current versus time under chopped irradiation of Fc-POPs at a bias voltage of 0 V (vs. Ag/AgCl). (b) Impedance (Z) versus time for Fc-POPs working electrodes that recorded in the darkness (green line) and under simulated sunlight irradiation (red line, light intensity= 0.3 W/cm²) at 0 V for 180 seconds ($f=1000$ Hz).

Density Functional Theoretical Calculations

All calculations were performed by the open source software CP2K package[41]. PBE functional attached D3 correction was used to describe the system [42]. In the framework of the Gaussian and plane waves method, Kohn-Sham DFT was utilized as the electronic structure method [43]. The Goedecker-Teter-Hutter (GTH) pseudopotentials, DZVP-MOLOPT-SR-GTH basis sets were used separately to describe the molecules [44, 45]. A plane-wave energy cut-off of 500 Ry and relative cut-off of 60 Ry have been employed. The energy convergence criterion was set as 10^{-6} Hartree. All molecules were contained in a $25 \times 25 \times 25 \text{ \AA}^3$ box under a periodic boundary condition. The free energy ΔG of each step for the whole reaction path could be calculated as follows Equation S4, and climbing image nudged elastic band method was used to find the transition state.

Equation S4: $\Delta G = \Delta E + (ZPE) - T\Delta S$

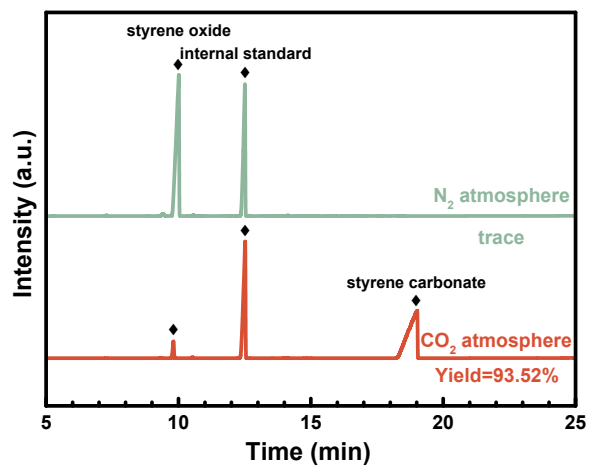


Fig S17. GC curves of the products after cycloaddition reaction under CO₂ atmosphere (red line) and N₂ atmosphere (green line). Other reaction conditions: 10 mg catalysts (Fc-POPs), 12.5 mmol styrene oxide (SO), 0.25 mmol TBAB, light intensity: 0.3 W/cm², pressure: 1 bar, 8 h.

References

1. H. Zhong, J. Gao, R. Sa, S. Yang, Z. Wu, R. Wang, *ChemSusChem*, 2020, **13**, 6323-6329.
2. S. Subramanian, J. Oppenheim, D. Kim, T. S. Nguyen, W. M. H. Silo, B. Kim, W. A. Goddard, C. T. Yavuz, *Chem.*, 2019, **5**, 3232-3242.
3. J. Chen, H. Li, M. Zhong, Q. Yang, *Green Chem.*, 2016, **18**, 6493-6500.
4. H. Zhong, Y. Su, X. Chen, X. Li, R. Wang, *ChemSusChem*, 2017, **10**, 4855-4863.
5. W. Hui, X. M. He, X. Y. Xu, Y. M. Chen, Y. Zhou, Z. M. Li, L. Zhang, D. J. Tao, *J. CO₂ Util.*, 2020, **36**, 169-176.
6. Y. Sang, J. Huang, *Chem. Eng. J.*, 2020, **385**, 123973.
7. W. Jiang, J. Yang, Y. Y. Liu, S. Y. Song, J.F. Ma, *Chem. Eur. J.*, 2016, **22**, 16991-16997.
8. Z. Dai, Y. Long, J. Liu, Y. Bao, L. Zheng, J. Ma, J. Liu, F. Zhang, Y. Xiong, J.Q. Lu, *Polymers (Basel)*, 2022, **14**, 2658.
9. J. Li, Y. Han, T. Ji, N. Wu, H. Lin, J. Jiang, J. Zhu, *Ind. Eng. Chem. Res.*, 2019, **59**, 676-684.
10. Q. Yu, Y. Z. Cheng, Z. Li, D. H. Yang, Q. Bo Meng, B. H. Han, *Chem. Eng. J.*, 2022, **442**, 136275.
11. X. Liao, B. Pei, R. Ma, L. Kong, X. Gao, J. He, X. Luo, J. Lin, *Catalysts*, 2022, **12**, 62.
12. Y. Qiu, Y. Chen, L. Lei, X. Wang, X. Zeng, Z. Feng, C. Deng, D. Lin, H. Ji, *Mol. Catal.*, 2022, **521**, 112171.
13. Y. Chen, Q. Ren, X. Zeng, L. Tao, X. Zhou, H. Ji, *Chem. Eng. Sci.*, 2021, **232**, 116380.
14. S. Ravi, P. Puthiaraj, D. W. Park, W. S. Ahn, *New J. Chem.*, 2018, **42**, 12429-12436.
15. H. Li, C. Li, J. Chen, L. Liu, Q. Yang, *Chem. Asian J.*, 2017, **12**, 1095-1103.
16. Z. Dai, Q. Sun, X. Liu, C. Bian, Q. Wu, S. Pan, L. Wang, X. Meng, F. Deng, F. S. Xiao, *J. Catal.*, 2016, **338**, 202-209.
17. J. Cao, W. Shan, Q. Wang, X. Ling, G. Li, Y. Lyu, Y. Zhou, J. Wang, *ACS Appl. Mater. Inter.*, 2019, **11**, 6031-6041.
18. J. Chen, M. Zhong, L. Tao, L. Liu, S. Jayakumar, C. Li, H. Li, Q. Yang, *Green Chem.*, 2018, **20**, 903-911.
19. M. Ding, H.L. Jiang, *Chem. Commun. (Camb)*, 2016, **52**, 12294-12297.
20. Y. Xie, R. X. Yang, N. Y. Huang, H. J. Luo, W. Q. Deng, *J. Energy Chem.*, 2014, **23**, 22-28.
21. N. Sharma, B. Ugale, S. Kumar, K. Kailasam, *Front. Chem.*, 2021, **9**, 737511.
22. Y. Xie, T.T. Wang, X.H. Liu, K. Zou, W.Q. Deng, *Nat. Commun.*, 2013, **4**, 1960.
23. F. Liu, S. Du, W. Zhang, J. Ma, S. Wang, M. Liu, F. Liu, *Chem. Eng. J.*, 2022, **435**, 134921.
24. X. Zhang, B. Qiu, Y. Zou, S. Wang, W. Mai, Y. Cao, Y. Wang, J. Chen, T. Li, *Micropor. and Mesopor. Mat.*, 2021, **319**, 110758.
25. J. Li, D. Jia, Z. Guo, Y. Liu, Y. Lyu, Y. Zhou, J. Wang, *Green Chem.*, 2017, **19**, 2675-2686.
26. X. Liao, X. Xiang, Z. Wang, R. Ma, L. Kong, X. Gao, J. He, W. Hou, C. Peng, J. Lin, *Sustain. Energ. Fuels*, 2022, **6**, 2846-2857.
27. X. Zhang, J. Wang, Y. Bian, H. Lv, B. Qiu, Y. Zhang, R. Qin, D. Zhu, S. Zhang, D. Li, S. Wang, W. Mai, Y. Li, T. Li, *J. CO₂ Util.*, 2022, **58**, 101924.
28. X. Zhang, J. Ding, B. Qiu, D. Li, Y. Bian, D. Zhu, S. Wang, W. Mai, S. Ming, J. Chen, T. Li, *ChemCatChem*, 2021, **13**, 2664-2673.
29. X. Zhang, H. Zhang, B. Qiu, D. Zhu, S. Zhang, Y. Bian, J. Wang, D. Li, S. Wang, W. Mai, J. Chen,

- T. Li, *Fuel*, 2023, **331**, 125828.
30. C. Cui, R. Sa, Z. Hong, H. Zhong, R. Wang, *ChemSusChem*, 2020, **13**, 180-187.
31. G. Li, X. Zhou, Z. Wang, *Micropor. Mesopor. Mat.*, 2022, **343**, 112119.
32. H. Ouyang, K. Song, J. Du, Z. Zhan, B. Tan, *Chem. Eng. J.*, 2022, **431**, 134326.
33. S. Z. Hu, Z. X. Xie, Z.H. Zhou, *Acta Phys. -Chim. Sin.*, 2010, **26**, 1795-1800.
34. S. Bhunia, R. A. Molla, V. Kumari, S. M. Islam, A. Bhaumik, *Chem. Commun. (Camb)*, 2015, **51**, 15732-15735.
35. M. H. Alkordi, Ł. J. Weseliński, V. D'Elia, S. Barman, A. Cadiou, M. N. Hedhili, A. J. Cairns, R. G. AbdulHalim, J. M. Basset, M. Eddaoudi, *J. Mater. Chem. A*, 2016, **4**, 7453-7460.
36. Z. Dai, Q. Sun, X. Liu, L. Guo, J. Li, S. Pan, C. Bian, L. Wang, X. Hu, X. Meng, L. Zhao, F. Deng, F. S. Xiao, *ChemSusChem*, 2017, **10**, 1186-1192.
37. X. Zhang, H. Liu, P. An, Y. Shi, J. Han, Z. Yang, C. Long, J. Guo, S. Zhao, K. Zhao, H. Yin, L. Zheng, B. Zhang, X. Liu, L. Zhang, G. Li, Z. Tang, *Sci. Adv.*, 2020, **6**, eaaz4824.
38. H. Li, X. Feng, P. Shao, J. Chen, C. Li, S. Jayakumar, Q. Yang, *J. Mater. Chem. A*, 2019, **7**, 5482-5492.
39. C. Sarkar, R. Paul, D. Q. Dao, S. Xu, R. Chatterjee, S. C. Shit, A. Bhaumik, J. Mondal, *ACS Appl. Mater. Inter.*, 2022, **14**, 37620-37636.
40. Y. Li, X. Song, G. Zhang, W. Chen, L. Wang, Y. Liu, L. Chen, *Sci. China Mater.*, 2021, **65**, 1377-1382.
41. J. Hutter, M. Iannuzzi, F. Schiffmann, J. VandeVondele, *WIREs: Comput. Mol. Sci.*, 2014, **4**, 15-25.
42. J. P. Perdew, K. Burke, M. Ernzerhof, *Phys. Rev. Lett.*, 1996, **77**, 3865-3868.
43. J. VandeVondele, M. Krack, F. Mohamed, M. Parrinello, T. Chassaing, J. Hutter, *Comput. Phys. Commun.*, 2005, **167**, 103-128.
44. S. Goedecker, M. Teter, J. Hutter, *Phys. Rev. B Condens. Matter*, 1996, **54**, 1703-1710.
45. C. Hartwigsen, S. Goedecker, J. Hutter, *Phys. Rev. B*, 1998, **58**, 3641-3662.